Mechanism and Kinetics of the Persulfate-Initiated Polymerization of Acrylamide

D. Hunkeler

Department of Chemical Engineering, Vanderbilt University, Nashville, Tennessee 37235

Received April 12, 1990; Revised Manuscript Received August 29, 1990

ABSTRACT: Acrylamide was polymerized at high monomer concentrations (25–50 wt %) at temperatures between 40 and 60 °C with potassium persulfate as the initiator. The rate of polymerization was found to be proportional to the monomer concentration to the $^5/_4$th power, a dependence extensively reported at low and moderate levels, suggesting that the rate order is invariant to the acrylamide concentration up to its solubility limit in water. Limiting conversions have also been observed and are reciprocally related to the initial monomer concentration. Both the high rate orders and limiting conversion are found to be manifestations of the same phenomena: the monomer-enhanced decomposition of potassium persulfate. A "hybrid cage–complex" mechanism, in which hydrogen bonding between the monomer and initiator lead to association, has been derived. This postulates that the monomer–initiator associate leads to donor–acceptor interactions between the amide and the persulfate. The decomposition of this charge-transfer complex leads to a secondary initiation reaction, which proceeds in competition with and often in preference to the thermal bond rupture of the peroxide. It will be shown to give good quantitative prediction of the polymerization rate order, monomer and initiator consumption, and molecular weight. Furthermore, the mechanism avoids the free-energy inconsistencies characteristic of prior theories and is generalizable to other nonionic and ionogenic acrylic water-soluble monomers in polar solvents.

Introduction

Polyacrylamide homopolymers derive their utility from their long chain lengths and expanded configuration in aqueous solutions. As such they are used primarily for water modification purposes. For example, drag reduction agents function by transferring energy from the eddies to provide a laminar flow regime and decrease the hydrolytic resistance. Polyacrylamides are also applied as thickening agents,[1] cutting fluids,[2] and soil stabilizers[3] and to a lesser extent in gel electrophoresis,[4] soaps,[5] and textile applications.[6] They are also used in emulsion or microemulsion form as cleaners and in enhanced oil recovery.[7] Recently, hydrophobic modifications have expanded the market for polyacrylamides. For commercial applications polyacrylamide quality is derived from its moisture insensitivity, oxidative stability,[8] and rapid dissolution in water.

Review of Kinetics

In 1967, Riggs and Rodriguez[9] observed an unusual rate dependence for aqueous acrylamide polymerizations initiated with potassium persulfate:

$$R_p = k[M]^{1.25}[I]^{0.5} \quad (1)$$

Over the past two decades, 22 investigations have confirmed a monomer dependency exceeding first order while maintaining that termination occurs predominantly through a bimolecular macroradical reaction.[10] Riggs and Rodriguez[11] interpreted the high rate order as evidence of monomeric influences on the rate of initiation. This had previously been postulated by Jenkins[12] to account for similar observations made while polymerizing styrene in toluene with benzoyl peroxide as an initiator. Morgan[13] had taken the inference a step further, suggesting his sesquimolecular order was attributable to secondary initiation caused by the monomer-enhanced decomposition of peroxide. The credibility of this hypothesis has been enhanced through experimental work performed by Dainton and co-workers.[14–17] They observed the rate dependence to revert to unity in the absence of chemical initiators. (Polymerizations were initiated with ^{60}Co γ-rays, which generated H and OH radicals, but left propagation, termination, and transfer reactions unchanged.) Further experimental evidence of the monomer-enhanced decomposition phenomena will be presented in a subsequent section of this paper.

To account for high rate orders with respect to monomer, three mechanisms have been proposed: the cage-effect theory (Matheson, 1946),[18] the complex theory (Gee and Rideal, 1936, 1939),[19,20] and the solvent-transfer theory (Burnett, 1955; Allen, 1955).[21,22] The latter assumes that the solvent acts as a unimolecular terminating agent. A necessary consequence is that the corresponding transfer radical is unreactive. However, in aqueous media the solvent-transfer mechanism is not a viable explanation for the high rate order phenomena since the hydroxy-transfer radical is very unstable and is capable of initiating olefinic monomers (Noyes, 1955).[23]

The complex theory assumes a reversible association complex is formed between the monomer and initiator. This decomposes to produce a primary radical and a macroradical of length one:

1. $$I + M \overset{K_c}{\rightleftharpoons} I\text{–}M$$

2. $$I\text{–}M \xrightarrow{k_i} R_1^{\bullet} + R_{in}^{\bullet}$$

Matheson's alternative explanation for the initiation mechanism assumes that as two fragments of a dissociated molecule are produced they are contained in a "cage" of solvent molecules. This radical pair may combine several times before diffusing out of the cage. This hypothesis is based on Eyring's (1940) observation[24] for benzene at room temperature, where a molecule made 10^{10} movements in its equilibrium position per second but underwent 10^{13-14} collisions in the same period. For the persulfate-initiated polymerization of acrylamide the cage-effect theory can be written as

0024-9297/91/2224-2160$02.50/0

1. $$I \underset{k_1'}{\overset{k_1}{\rightleftharpoons}} (R_{in}^{\bullet}\ {}^{\bullet}R_{in})$$

2. $$(R_{in}^{\bullet}) \xrightarrow{k_D} R_{in}^{\bullet}$$

3. $$2R_{in}^{\bullet} \xrightarrow{k_r} I$$

4. $$(R_{in}^{\bullet}\ {}^{\bullet}R_{in}) + M \xrightarrow{k_{MI}} R_1^{\bullet} + R_{in}^{\bullet}$$

Although, based on very different premises, both these mechanisms reduce to an identical rate equation

$$R_p = \frac{k_p}{k_t^{1/2}}[I]^{1/2}[M]^{3/2}(2k_i)^{1/2}\left(\frac{K}{1+K[M]}\right)^{1/2} \quad (2)$$

where k_i is the complex/initiator decomposition constant for the complex and cage theories, respectively, and K is the complex association constant (K_c) or the ratio k_{MI}/k_r, which represents the relative rate at which a caged radical undergoes propagation and recombination.

These predict an increase in the rate order from 1.0 to 1.5 as the conversion increases. While either mechanism can satisfactorily predict the conversion-time development for acrylamide polymerizations,[25] there has been no direct verification that the order is changing with monomer concentration. This has caused concern that neither mechanism is representative of actual physical phenomena. Furthermore, since both theories reduce to the same rate equation, kinetics cannot be used to discriminate between the mechanisms. In the following section, we will therefore evaluate the cage and complex mechanisms on the basis of thermodynamic consistency and nonkinetic experimental observations.

Evaluation of the Cage-Effect and Complex Theories. Flory (1953) has shown that for typical values of radical diffusivities (10^{-5} cm^2/s) the monomer cannot appreciably influence the events in the cage.[26] That is, the enhanced decomposition of caged radicals is insignificant relative to diffusion out of the cage, unless, as Jenkins showed,[12] the cage has enormous dimensions (10^4-Å radius), which seems improbable. The theory does, however, predict low efficiencies of initiation,[27] and these have been reported for aqueous acrylamide polymerizations (f = 0.024).[28]

Noyes[23] broadened the scope of the cage-effect theory by developing a hierarchal cage structure. He defined the following: primary recombination, between two molecular fragments that are separated by less than one molecular diameter; secondary recombination, between two fragments of the same molecule that have diffused greater than one molecular diameter apart; tertiary recombination, between two fragments from different initiator molecules. Primary and secondary recombinations occur in $\approx 10^{-13}$ and 10^{-9} s, respectively. Since the time between diffusive displacements is approximately 10^{-11} s, monomer-enhanced decomposition cannot compete with primary recombination. However, if the scavenger (monomer) concentration is high, Noyes calculated that the fraction of radicals reacting with scavenger that would otherwise have undergone secondary recombination is, to the first approximation, proportional to $[M]^{1/2}$. That is

$$R_I \propto [M]^{1/2} \quad (3)$$

which accounts for the observed rate behavior for acrylamide polymerizations, i.e., $R_p \propto M^{1.25}$.

Noyes' calculations suggest that although monomer–cage interactions are insignificant for cages with short lifetimes, for the fraction of cages where radicals are significantly separated, the enhanced decomposition reactions are competitive. Furthermore, the long cage lifetimes necessary for enhanced decomposition suggest that if the cage theory is true, Flory and Jenkins have overestimated the macroradical diffusion coefficient. Noyes' theoretical calculation is equivalent to the kinetic approach we will develop in this paper. Specifically, we will define the existence of two cage entities: "compact", where the radicals are separated by less than one molecular diameter and "diffuse" where they have diffused further apart. It is postulated that only the latter are susceptible to monomer attack. This is an oversimplification, as physically there is a continuous distribution of cage sizes (radical separations). However, from a mechanistic viewpoint, there is a critical radical separation, which, if achieved, allows the monomer to compete with radical fragment recombination. Therefore, the population can be divided into two regimes according to their reactivity.

Complex Theory. The complex theory has been historically criticized and rejected because experimental data indicate that the association constant rises with temperature. This is inconsistent with energetic predictions, which indicate the complex is less favorable at higher temperatures. Further indirect evidence against amide–persulfate complexability was presented by Riggs and Rodriguez,[9] who showed the overall activation energy for aqueous acrylamide polymerization (16 900 cal/mol) was almost exclusively composed of the contribution from the thermal decomposition of potassium persulfate ($E_{kd/2}$ = 16 800 cal/mol; complex formulation should reduce the activation energy). However, more recent experiments[29] indicate that the overall activation energy is appreciably lowered, to below 10 kcal/mol in the presence of monomer. In the same investigation ultraviolet spectrometry was used to identify new complexes produced when acrylonitrile and *N*-vinylpyrrolidone, two nitrogen containing monomers, were mixed with potassium persulfate. Furthermore, the optical intensity of the new bands reached a maximum at a time coincident with the induction period of the reaction. The authors concluded a donor–acceptor complex was produced between the nitrogen-containing monomer and the persulfate (Trubitsyna, 1966).[30] These authors also attributed the color change, noticeable immediately after mixing nitrogen-containing monomers and persulfates, to the formation of a molecular complex. Further evidence to this end came from polymerizations with monomers that are stronger proton donors than acrylonitrile and *N*-vinylpyrrolidone: styrene, methyl methacrylate, isoprene, and methyl acrylate. When these are added to persulfate, no polymerization occurs although iodometrically the concentration of potassium persulfate decreases by 70% in the first hour. These monomers are preferentially forming a complex with potassium persulfate and blocking out the nitrogen-containing monomers. This is significant in three respects: first, it shows that the new bands in the UV spectrum cannot be attributable to nonmonomeric species, such as oxygen; second, it demonstrates that proton donation from the monomer to the persulfate is a prerequisite for enhanced decomposition; third, it implies that the complex *is* initiating polymerization, since potassium persulfate alone at 20 °C is incapable of initiating the reaction.

Other peroxide initiators (benzoyl peroxide: Trubitsyna, 1965)[31] have also been shown to decompose at faster rates in the presence of nitrogen-containing additives. In this case the enhanced decomposition was also accompanied

by a decrease in the overall activation energy. This was observed by the same authors several years later for reactions between benzoyl peroxide and aminated polystyrene,[32] indicating that the donor–acceptor interactions are not dependent on molecular architecture.

In 1978, Trubitsyna[33] used conductivity to monitor the charged particles produced from the interaction of acrylamide and potassium persulfate. These experiments found the onset of charged particle generation corresponded to the induction period of the reaction and the onset of radical generation, as determined by ESR. Furthermore, they were performed below 20 °C, where the thermal decomposition of potassium persulfate is negligible, indicating a secondary decomposition reaction was occurring. On the basis of these observations, Trubitsyna[33] proposed an electron donor mechanism, with concurrent radical and charge generation.

Morsi[34] observed that diphenylamine enhanced the decomposition of benzoyl peroxide. He also attributed this to a donor–acceptor interaction between the amine and the peroxide and suggested the interaction was caused by a modification of the peroxide's dihedral angle. Further evidence that acrylamide associates with potassium persulfate comes from Bekturov,[35] who found SO_4^{2-} salted out poly(vinylpyrrolidone) but could not precipitate polyacrylamide, presumably because it was neutralized by a reaction with the amide side chains. The reaction of amides with persulfate is not surprising in light of NMR evidence[36] that shows that the carbonyl groups are hydrogen bonded to water but the amides are relatively free. Coleman[37] has confirmed that the carbonyl and amide substituents behave complementarily in that the binding of one functional group is concurrent with the reactivity of the second.

Chapiro[38] conducted an extensive investigation of the solvent effects on acrylamide polymerization and reported:

$$R_{p,water} > R_{p,acetic\ acid} > R_{p,methanol} > R_{p,DMF} \approx R_{p,dioxane} \approx R_{p,toluene} > R_{p,acetonitrile} \quad (4)$$

These strong effects have been shown to be due to the polarity and hydrogen-bonding affinity of acrylamide. Gromov[39] studied acrylamide polymerization in water, DMSO, and THF and concluded that as the polarity of the solvent rises its ability to donate protons to the carbonyl rises. This results in a positive charge on the amide and an increased electron localization on the α-carbon. These observations will be shown to be consistent with a kinetic model developed in a subsequent section of this paper. Bune et al.[40] have confirmed, by ^1H and ^{13}C NMR, that hydrogen bonding occurs predominantly through the carbonyl group ($\delta_{C=O}$ shifts to weaker field positions while δ_{NH_2} is essentially unchanged). They also correlated the electron-accepting ability of the carbonyl with an increased electron density on the conjugated double bond.

Manickam[41] has also developed a mechanism where monomer-enhanced decomposition is included outside the framework of cage or complex theories, but this also assumes a 100% efficiency for monomer-enhanced decomposition, limiting its utility.

The following conclusions ensue from the preceding discussion and serve as a basis for the derivation of a synthesis mechanism and kinetic model:

(1) Monomers containing highly electronegative substituents can form "associates" with peroxide-containing initiators. This enhances the decomposition of, for example, potassium persulfate, at low temperatures, reducing the activation energy and extending the useful range of the initiator.

(2) The electrical environment of the monomer is the primary factor in its interaction with peroxide.

(3) Monomer-enhanced decomposition is limited to initiator molecules where the radical pair has achieved a minimum "critical" separation.

(4) The enhanced decomposition of complexed persulfate is caused by hindered recombination and not a greater frequency of fragment dissociations. When the initiator is bound to the monomer, the dissociated radical pair cannot regenerate potassium persulfate by recombination. Either radicals or an inert recombination product of the form $O^{\bullet-}SO_3MO_3SO^{\bullet-}$ are produced. Therefore, in the presence of donor–acceptor interactions, each radical separation or "transient dissociation" results in the consumption of one initiator molecule. In the absence of bound monomer, an initiator transiently decomposes and recombines 10^{2-3} times for each "permanent decomposition".

Elucidation of an Initiation Mechanism

Complex–Cage Equivalence. We have shown in the preceding section that the formation of an intermediate "associate" is a necessary precursor to monomer-enhanced decomposition. This allows the electron-donating group sufficient time to attack the peroxide to be competitive with the rapid radical fragmentation and recombination reactions. This monomer–initiator associate can result from either the diffusive displacement of a monomer to the volume element of the peroxide (cage approach) or the formation of a molecular complex. Both of these phenomena can be represented by a general reaction that is nonspecific to the forces drawing the monomer and initiator into close proximity. (This modification must also be applied to Manickam's mechanism to successfully apply it.)

$$\{R_{in}^{\bullet}\ {}^{\bullet}R_{in}\} + M \rightarrow \left\{R_{in}^{\bullet} \underset{M}{+} R_{in}^{\bullet}\right\} \quad (5)$$

That is, the "associate" is a broadly defined concept encompassing both covalent and weak-bonding interactions. However, since experimental measurements[33] have found the associate to be irreversibly and nonspontaneously formed, uncharacteristic of covalently bonded molecules, a weak-bonding interaction must be responsible for monomer–initiator association. This "associate" can therefore be represented as a "weak complex", formed presumably due to hydrogen bonding, or equivalently, as a "diffuse monomer swollen cage", the difference being entirely semantic since in both models the monomer is physically contained within the three-dimensional volume element of a diffuse radical pair. In other words, the complex and cage treatments are nondiscriminating models of the same physical phenomena as far as amide–persulfate interactions are concerned. The forces responsible for the formation of the associate will be discussed in a subsequent section of the paper following a presentation of the reaction mechanism.

The ambiguity in defining cage or complex structures allows us to combine the positive features of both mechanisms. Specifically, Noyes' hierarchical cage structure will be used as a precursor to association and charge-transfer reactions. This will allow the implementation of a monomer-enhanced decomposition mechanism without the inconsistency of association phenomena increasing with temperature, the main drawback of existing mechanisms. For obvious reasons, the new mechanism will be referred to as the "hybrid cage–complex" or "hybrid" mechanism and is developed below.

Proposed Mechanism. The apparent increase in the association constant (k_a) with temperature can be rationalized if we consider association, and the donor–acceptor reactions, to proceed within the framework of a caged mechanism. Reactions of the sulfate radical that generate nonreactive products must also be included to account for low efficiencies of initiation (f = 0.06–0.4).

Initiator Reactions (Formation of a Caged Hierarchy).

1. $S_2O_8^{2-} \underset{k_1'}{\overset{k_1}{\rightleftharpoons}} (SO_4^{\bullet-}\cdots{}^{\bullet}O_4S)$

2. $(SO_4^{\bullet-}\cdots{}^{\bullet}O_4S) \xrightarrow{k_2} \{SO_4^{\bullet-}\cdots{}^{\bullet}O_4S\}$

3. $\{SO_4^{\bullet-}\cdots{}^{\bullet}O_4S\} \xrightarrow{k_d^*} 2SO_4^{\bullet-}$

4. $\{SO_4^{\bullet-}\cdots{}^{\bullet}O_4S\} \xrightarrow{k_r} S_2O_8^{2-}$

Parentheses indicate a "compact cage" and braces signify a "diffuse cage".

Swollen Cage Formation ("Association") and Decomposition.

5. association

$$\{SO_4^{\bullet-}\cdots{}^{\bullet}O_4S\} + M \xrightarrow{k_a^*} \left\{SO_4^{\bullet-}\underset{M}{\cdots}{}^{\bullet}O_4S\right\}$$

6. dissociation through a donor–acceptor intermediate

$$\left\{SO_4^{\bullet-}\underset{M}{\cdots}{}^{\bullet}O_4S\right\} \xrightarrow{k_b} SO_4^{\bullet-} + HSO_4^- + CH_2C^{\bullet}C(O)NH_2$$

7. $\left\{SO_4^{\bullet-}\underset{M}{\cdots}{}^{\bullet}O_4S\right\} \xrightarrow{k_c} Q$ (inert products)

Step 7 represents the consumption of monomer–initiator associates through a reaction that generates nonreactive products. This initiator deactivation is necessary to avoid nonunit efficiencies of initiation.

Chain Initiation.

8. $SO_4^{\bullet-} + M \xrightarrow{k_{i1}} R_1^{\bullet}$

Bunn[42] has shown that sulfate radicals can also react with water to produce hydroxy radicals, which are capable of initiation.[43]

9. $SO_4^{\bullet-} + H_2O \xrightarrow{k_H} HSO_4^- + {}^{\bullet}OH$

10. ${}^{\bullet}OH + M \xrightarrow{k_{i2}} R_1^{\bullet}$

Propagation.

11. $R_r^{\bullet} + M \xrightarrow{k_p} R_{r+1}^{\bullet}$

Transfer to Monomer.

12. $R_r^{\bullet} + M \xrightarrow{k_{tm}} P_r + R_1^{\bullet}$

Termination.

13. $R_r^{\bullet} + R_s^{\bullet} \xrightarrow{k_{td}} P_r + P_s$

Kinetic Model

At any time t, the persulfate is comprised of undissociated initiator ($S_2O_8^{2-}$), "compact caged fragments" ($SO_4^{\bullet-}\cdots{}^{\bullet}O_4S$), and "diffuse cage fragments" $\{SO_4^{\bullet-}\cdots{}^{\bullet}O_4S\}$. The total persulfate in the system (I_t) is

$$I_t = [S_2O_8^{2-}] + (SO_4^{\bullet-}\cdots{}^{\bullet}O_4S) + \{SO_4^{\bullet-}\cdots{}^{\bullet}O_4S\} \quad (6)$$

where

$$[S_2O_8^{2-}] = \Phi_0 I_t$$

$$(SO_4^{\bullet-}\cdots{}^{\bullet}O_4S) = \Phi_1 I_t$$

$$\{SO_4^{\bullet-}\cdots{}^{\bullet}O_4S\} = \Phi_2 I_t$$

and $\Phi_0 + \Phi_1 + \Phi_2 = 1.0$.

The balances on all reactive species follow:

$$\frac{d[S_2O_8^{2-}]}{dt} = -k_1[S_2O_8^{2-}] + k_1'(SO_4^{\bullet-}\cdots{}^{\bullet}O_4S) + k_r\{SO_4^{\bullet-}\cdots{}^{\bullet}O_4S\} \quad (7)$$

$$\frac{d(SO_4^{\bullet-}\cdots{}^{\bullet}O_4S)}{dt} = k_1[S_2O_8^{2-}] - (k_1' + k_2)(SO_4^{\bullet-}\cdots{}^{\bullet}O_4S) \quad (8)$$

$$\frac{d\{SO_4^{\bullet-}\cdots{}^{\bullet}O_4S\}}{dt} = k_2(SO_4^{\bullet-}\cdots{}^{\bullet}O_4S) - k_d^*\{SO_4^{\bullet-}\cdots{}^{\bullet}O_4S\} - k_r\{SO_4^{\bullet-}\cdots{}^{\bullet}O_4S\} - k_a^*\{SO_4^{\bullet-}\cdots{}^{\bullet}O_4S\}[M] \quad (9)$$

$$\frac{d\left\{SO_4^{\bullet-}\underset{M}{\cdots}{}^{\bullet}O_4S\right\}}{dt} = k_a^*\{SO_4^{\bullet-}\cdots{}^{\bullet}O_4S\}[M] - (k_b + k_c)\left\{SO_4^{\bullet-}\underset{M}{\cdots}{}^{\bullet}O_4S\right\} \approx 0 \quad (10)$$

$$\frac{d(SO_4^{\bullet-})}{dt} = 2k_d^*\{SO_4^{\bullet-}\cdots{}^{\bullet}O_4S\} + k_b\left\{SO_4^{\bullet-}\underset{M}{\cdots}{}^{\bullet}O_4S\right\} - k_H[SO_4^{\bullet-}][H_2O] - k_{i1}[SO_4^{\bullet-}][M] \approx 0 \quad (11)$$

$$\frac{d[{}^{\bullet}OH]}{dt} = k_H[SO_4^{\bullet-}][H_2O] - k_{i2}[{}^{\bullet}OH][M] \approx 0 \quad (12)$$

$$\frac{d[R^{\bullet}]}{dt} = k_{i1}[SO_4^{\bullet-}][M] + k_{i2}[{}^{\bullet}OH][M] + k_b\left\{SO_4^{\bullet-}\underset{M}{\cdots}{}^{\bullet}O_4S\right\} - k_{td}[R^{\bullet}]^2 \approx 0 \quad (13)$$

From eq 10

$$\left\{SO_4^{\bullet-}\underset{M}{\cdots}{}^{\bullet}O_4S\right\} = \left(\frac{k_a^*}{k_b + k_c}\right)\{SO_4^{\bullet-}\cdots{}^{\bullet}O_4S\}[M] \quad (10')$$

Assuming k_p is independent of chain length ($k_{i1} = k_{i2} = k_p$), eqs 10′, 11, and 12 can be substituted into eq 13 to yield

$$[R^{\bullet}] = \left(\frac{2fk_d^*\{SO_4^{\bullet-}\cdots{}^{\bullet}O_4S\}}{k_{td}} + \frac{2f_c k_a^*\{SO_4^{\bullet-}\cdots{}^{\bullet}O_4S\}[M]}{k_{td}}\right)^{1/2}$$

where

$$\{SO_4^{\bullet-}\cdots{}^{\bullet}O_4S\} = \Phi_2(S_2O_8^{2-})$$

and

$$f_c = \frac{1}{1 + k_c/k_b}$$

where f_c can be defined equivalently as a cage destruction of complex-decomposition efficiency.

The long chain approximation subsequently yields

$$R_p = k_p[M] \times \left(\frac{2f(\Phi_2 k_d^*)[S_2O_8^{2-}]}{k_{td}} + \frac{2f_c(\Phi_2 k_a^*)[S_2O_8^{2-}]}{k_{td}}[M]\right)^{1/2} \quad (14)$$

Discussion of the Derived Rate Equation. The decomposition constant (k_d) has been determined from measurements of the concentration of undecomposed initiator:[44]

$$\frac{d[S_2O_8^{2-}]}{dt} = -k_d[S_2O_8^{2-}] \quad (15)$$

However, since only diffuse cage fragments can dissociate to produce unpaired free radicals, eq 15 can more appropriately be written as

$$\frac{d[S_2O_8^{2-}]}{dt} = k_d^*\{SO_4^{\bullet-}\cdots{}^{\bullet}O_4S\} \quad (16)$$

Expressing the concentration of these diffuse cages as a fraction of the overall initiator level, eqs 15 and 16 can be combined to yield

$$\frac{d[S_2O_8^{2-}]}{dt} = \Phi_2 k_d^*[S_2O_8^{2-}]$$

which provides the identity $k_d = \Phi_2 k_d^*$. By an analogous procedure it can be shown that $k_a = \Phi_2 k_a^*$, where k_a is the apparent (overall) association constant and k_a^* is the actual (specific) association constant.

As the thermal energy of the system increases, the frequency of equilibrium displacement of small molecules rises and the probability of recombination decreases. If we interpret this in terms of initiator reactions, the radical pairs formed through the transient dissociation of the initiator molecules will achieve greater molecular separation and have longer lifetimes prior to recombination. In the context of the hierarchical cage mechanism developed herein, this is represented as an increase in the fraction of diffuse cages (Φ_2) at the expense of a reduced concentration of compact cages (Φ_1). The utility of the hybrid mechanism is therefore immediately obvious. At increased temperatures the apparent association constant (k_a) has been observed to rise. This is *not* due to an actual increase in association phenomena (k_a^*), which is energetically unfavorable, but rather to an increase in the fraction of radical species with sufficient separation to participate in association reactions (Φ_2 increases). Such thermodynamic consistency in the kinetic model is not possible without hybridizing the cage-effect and complex theories, specifically using a caged precursor to association and donor–acceptor interactions. This represents the major improvement of the hybrid mechanism over the existing theories.

The hybrid mechanism is further characterized by two competing initiation processes: thermal bond rupture and monomer-enhanced decomposition. These yield the following rate equations.

thermal decomposition dominates:

$$R_p = k_p[M]\left(\frac{2fk_d[I]}{k_{td}}\right)^{1/2}$$

monomer-enhanced decomposition dominates:

$$R_p = k_p[M]^{3/2}\left(\frac{2f_c k_a[I]}{k_{td}}\right)^{1/2}$$

Table I
Equivalence of Two Kinetic Processes Which Provide $^5/_4$th Power Rate Dependencies

monomer concn [M]	$R_p = k_1[M]^{1.25}$ [a]	$R_p = k_1([M] + [M]^{1.5})/2$ [a]
0.5	0.42	0.43
1.0	1.0	1.0
2.0	2.38	2.41
3.0	3.95	4.10
4.0	5.66	6.00
5.0	7.48	8.09
6.0	9.39	10.34
7.0	11.39	12.76

[a] k_1 is assigned an arbitrary value of 1.0.

The overall polymerization rate order with respect to monomer concentration is therefore governed by the relative rates of thermal decomposition (k_d) and association (k_a) and their respective initiation efficiencies (f, f_c). Indeed the hybrid mechanism predicts a direct correspondence exists between the strength of the monomer–initiator association and the rate order, which lies between 1.0 and 1.5. If the mechanism is correct, it implies that the observed $^5/_4$th power for acrylamide polymerizations is actually an "apparent" order, with the true kinetic process being a relatively equal balance between unimolecular and sesquimolecular reaction mechanisms (thermal and monomer-enhanced decomposition). Table I shows rate data generated from the hybrid mechanism (eq 14) with arbitrary parameter values. These are virtually indistinguishable from kinetics generated with a single $^5/_4$th order term. Therefore, on the basis of kinetic observations, it cannot be ascertained whether the unique 1.25 rate order for acrylamide is due to a single initiation mechanism or competition between multiple processes of unit and sesquimolecular order. The hybrid mechanism cannot be refuted on kinetic bases and must be evaluated using nonkinetic criteria, such as the free-energy analysis in the preceding paragraph.

Generalization of the Initiation Mechanism to Other Water-Soluble Monomers

The charge-transfer complexes that form between persulfate- and nitrogen-containing monomers require free electrons on the donor (monomer) and a polar medium. For acrylamide polymerizations in dimethyl sulfoxide–water mixtures, the rate order with respect to monomer increases as the fraction of DMSO in the solvent mixture rises.[45,46] This is caused by the aprotic nature of dimethyl sulfoxide and its inability to hydrogen bond to the acrylamide carbonyl group. This less solvated monomer is therefore more readily complexed with the peroxide and undergoes enhanced decomposition at an accelerated rate. The rate therefore approaches sesquimolecular order, the limit if monomer and initiator form 1:1 complexes, as the fraction of DMSO rises, in agreement with experimental observations.

This effect is also observed in other monomers with electronegative atoms, for example, in acrylic acid (oxygen)–persulfate systems.[41] The polarity and hydrogen-bonding affinity of the hydroxy group exceed that of the corresponding amide, and the rate order again approaches the sesquimolecular limit. Indeed, the monomer's ability to form hydrogen bonds, through the side-chain functional group, appears to be the principal cause of association with peroxide-containing initiators.

For *N*,*N*-dimethylacrylamide, which cannot hydrogen bond to either the peroxide or persulfate oxygens, due perhaps to steric interference of the bulky methyl substituents, association phenomena and monomer-enhanced

Table II
Rate Equations for Several Acrylic Water-Soluble Monomers

monomer	"a" in $R_p \propto M^a$	ref
N,N-dimethylacrylamide	1.0	Kurenkov, 1980[54]
methacrylamide	1.13	Gupta, 1987[51]
acrylylglycinamide	1.22	Haas, 1970[50]
acrylamide	1.25	Riggs and Rodriguez, 1967[9]
acrylic acid	1.50	Manickam, 1979[41]
diallyldimethylammonium chloride	2.0[a]	Jaeger, 1984[55] Hahn, 1983[56,57]

[a] A third-order dependence has been reported. However, the monomeric salt influences propagation between charged radicals and monomer molecules. This results in a first-order relationship between the propagation rate constant and the monomer concentration.

decomposition are *not* observed and the rate order reverts to unity.[47,48] Ergozhin[49] investigated the kinetics of a series of N-substituted amides and observed the rate order with respect to monomer concentration to decrease as the accessibility to the vinyl group was hindered. This confirms Trubitsyna's postulate[33] that the amide is responsible for the electron rearrangement leading to the monomer–initiator association. Haas[50] has observed that other amide-containing monomers, for example, acrylylglycinamide, enhance the decomposition of potassium persulfate and have the same rate order with respect to monomer concentration as acrylamide, which is again consistent with a hydrogen-bonded associate. If methacrylamide replaces acrylamide as the monomer in a persulfate reaction, a greater than first-order dependence is again observed ($R_p \propto M^{1.13}$; Gupta, 1987).[51] The reduced order from the $^5/_4$th power may be an experimental anomaly, as methacrylamide has not been extensively investigated. However, it is more likely that the α-methyl substitution is affecting the electron arrangement necessary to produce a monomer–initiator complex.[52] (Methacrylamide radicals are present in a resonance-stabilized structure where the β-carbon can more easily stabilize a radical than the α-methyl-substituted carbon.[53])

Table II summarizes the observed kinetic relationships for several acrylic water-soluble monomers (acrylamide, acrylylglycinamide, acrylic acid, *N,N*-dimethylacrylamide, methacrylamide). There is a direct correspondence between the monomer's hydrogen-bonding affinity and the rate order with respect to monomer concentration. During the derivation of the hybrid cage–complex initiation mechanism, it was shown that high rate orders occurred concomitant with monomer–initiator association. If we combine these two observations, then the hybrid mechanism infers that hydrogen bonding between the monomer and persulfate is the cause of association phenomena. This seems intuitively reasonable and is quite probable.

The sum of a first- and sesquimolecular-order initiation mechanism, the hybrid cage–complex model, is therefore flexible enough to quantitatively describe a broad array of kinetic observations for nonionic and anionic acrylic water-soluble monomers. The stronger the hydrogen bonding between the monomer and persulfate, the greater the strength and extent of association and a larger proportion of initiator decomposes through a monomer-enhanced reaction (higher rate order). Contrarily, steric interferences shield the hydrogen bonding and hinder the ability to form charge-transfer complexes. This results in a larger fraction of the persulfate, which decomposes through a thermal bond rupture mechanism (rate order approaches unity).

Generalization to Cationic Monomers. Friend and Alexander[58] were the first to observe an interaction between persulfate and quaternary ammonium compounds. Trubitsyna[29,33,59] and Kurenkov[54] later observed complexes and enhanced decomposition of persulfate due to cationic ammonium additives. Further, the magnitude of the enhanced decomposition was significantly greater than was observed for acrylamide. It has been shown[58] that charge-transfer interactions are responsible for the formation of a 1:2 stoichiometric complex of the following type:

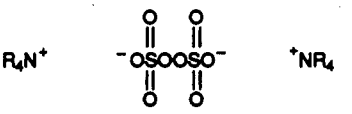

These decompose to produce two macroradicals of length 1 (when 1:1 complexes are produced, one primary radical is liberated). Such a mechanism reduces to a second-order rate dependence on monomer concentration, in agreement with experimental observations for diallyldimethylammonium chloride polymerization (Jaeger, 1984).[55] Jaeger also showed that the rate order was reduced by 1 when a noncomplexing initiator [azobis(pentanoic acid)] was used in place of potassium persulfate. Therefore, the high rate orders observed for polymerization of acrylic water-soluble monomers in aqueous media initiated by persulfate are almost certainly due to hydrogen-bonding and ionic interactions between the monomer–initiator pair. The strength in this interaction determines the deviation in order from unity. Table II summarizes the observed kinetic relationships for several nonionic, anionic, and cationic acrylic water-soluble monomers. A correlation between the rate order with respect to monomer and the strength of the monomer–initiator complex is again observable.

On the basis of the preceding literature survey, we can propose the following general initiation mechanism for acrylic water-soluble monomers with persulfate:

1. $S_2O_8^{2-} \rightleftharpoons (SO_4^{\bullet-}\cdots{}^{\bullet}O_4S)$
2. $(SO_4^{\bullet-}\cdots{}^{\bullet}O_4S) \rightarrow \{SO_4^{\bullet-}\cdots{}^{\bullet}O_4S\}$
3. $\{SO_4^{\bullet-}\cdots{}^{\bullet}O_4S\} \rightarrow S_2O_8^{2-}$
4. $\{SO_4^{\bullet-}\cdots{}^{\bullet}O_4S\} \rightarrow 2SO_4^{\bullet-}$
5. $SO_4^{\bullet-} + H_2O \rightarrow HSO_4^- + {}^{\bullet}OH$
6. $SO_4^{\bullet-} + M \rightarrow R_1^{\bullet}$
7. ${}^{\bullet}OH + M \rightarrow R_1^{\bullet}$
8. $(SO_4^{\bullet-}\cdots{}^{\bullet}O_4S) + xM \rightarrow \left\{SO_4^{\bullet-}{}_{xM}{}^{\bullet}O_4S\right\}$
9. $\left\{SO_4^{\bullet-}{}_{xM}{}^{\bullet}O_4S\right\} \rightarrow (2-x)R_{in}^{\bullet} + xR_1^{\bullet}$
10. $\left\{SO_4^{\bullet-}{}_{xM}{}^{\bullet}O_4S\right\} \rightarrow Q$ (inert products)

where x is the stoichiometric ratio of monomer in the initiator complex. That is, for anionic and nonionic monomers, $x = 1$ and $R_p \propto kM + k'M^{3/2}$, and for cationic monomers, $x = 2$ and $R_p \propto kM + k''M^2$.

An oppositely charged monomer–initiator pair is therefore able to form higher stoichiometric complexes than if the initiator and monomer are of the same charge, or if one or both of the species are uncharged. This accounts for the higher order in rate with respect to monomer

Table III
Polymerization Conditions

temp, °C	[acrylamide], mol/L	$[K_2S_2O_8]$, mmol/L	mass of aqueous phase, g	mass of Isopar-K, g	mass of SMS,[a] g
50	3.35	0.252	1000.0	1000.0	100.0
50	4.03	0.228	1000.0	1000.3	100.0
50	4.69	0.251	1000.0	999.9	100.0
50	5.37	0.248	1000.0	1000.0	100.0
50	6.04	0.250	1000.0	1002.1	99.9
50	6.41	0.238	1000.0	1000.3	100.0
40	6.70	1.573	1000.0	1000.2	100.0
60	6.70	0.0609	1000.0	1000.6	100.0

[a] Sorbitan monostearate.

Table IV
Limiting Conversion versus Monomer and Initiator Concentration

limiting conversion (X_1)	acrylamide concn, mol/L	potassium persulfate concn, mmol/L
0.92	6.41	0.238
0.95	6.04	0.250
0.96	5.37	0.248
0.996	4.69	0.251
0.996	4.03	0.228
0.997	3.35	0.252
0.76	6.70	0.0609
0.999	6.70	1.573

Table V
Parameter Estimates

param	value	units
f_c	40 °C: 1.0 50 °C: 0.372 60 °C: 0.065	dimensionless
$(\Phi_2 k_a^*)^a$	40 °C: 3.17×10^{-5} 50 °C: 1.06×10^{-3} 60 °C: 1.93×10^{-2}	L/mol·min
k_{fE}	2.433×10^{-9}	dm³/mol·min
$A_0{}^b$	8.01	dimensionless
$A_1{}^b$	2.0×10^{-2}	K^{-1} (Kim and Hamielec, 1984)

[a] $k_a = (\Phi_2 k_a^*) = 8.77 \times 10^{41} \exp(-66500/RT)$. [b] A is a gel effect parameter in the expression $k_{td}^0/k_{td} = \exp(Awp)$ where $A = A_0 - A_1 T$.

concentration for aqueous polymerizations of cationic monomers with persulfate.

Proposed Experimental Investigation

The hybrid mechanism predicts that the rate order with respect to monomer is exclusively a function of the chemical interactions between the monomer–initiator pair, hydrogen bonding for the acrylamide/persulfate/water system. This implies that the rate order is independent of reaction conditions, for example, the monomer concentration. (The cage-effect and complex theories predict a decrease in the rate order with monomer concentration.) This, however, cannot be verified from existing experimental observations,[10] which are limited to acrylamide levels below 30 wt %. A series of polymerizations are therefore planned between 25 and 50 wt % monomer, the latter delineated by the solubility of acrylamide in water. The suitability of the hybrid mechanism to describe the kinetics at high conversion and the molecular weight will also be determined.

Experimental Section

Conversions were inferred from measurements of the residual monomer concentration by high performance liquid chromatography. This method has been described in detail[60,61] and is

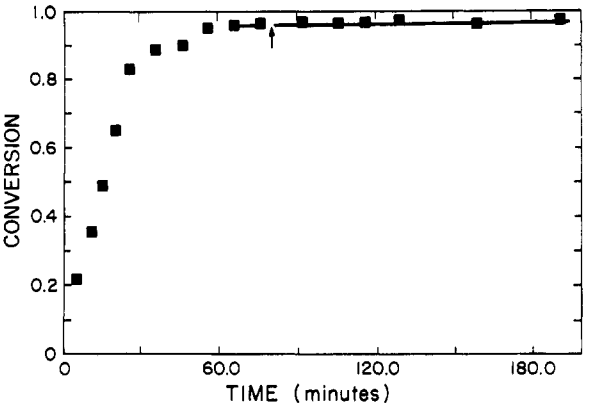

Figure 1. Conversion–time data (■) for an acrylamide polymerization. The experimental conditions were [monomer] = 5.37 mol/L_w, $[K_2S_2O_8] = 2.44 \times 10^{-3}$ mol/L_w, and temperature = 50 °C. A limiting conversion of 0.97 is observed. Increasing the temperature to 60 °C (arrow) did not lead to consumption of additional monomer.

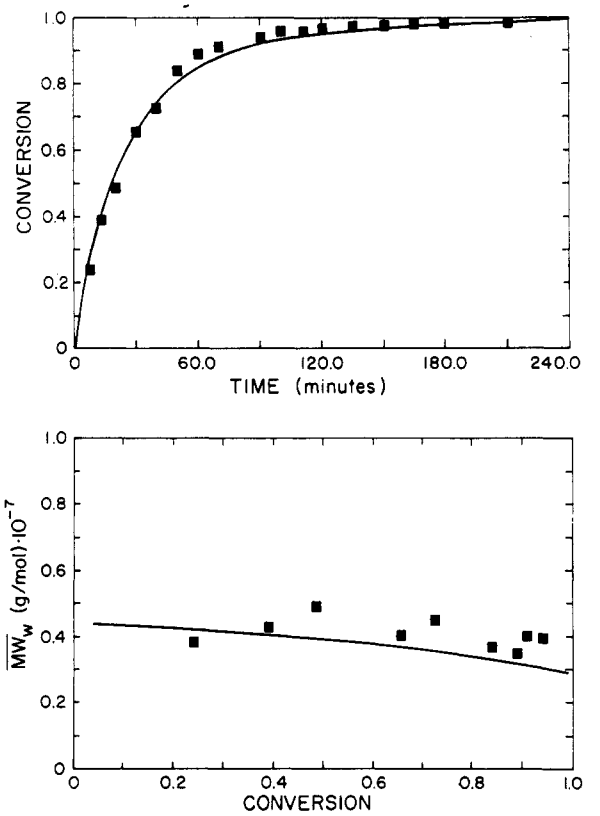

Figure 2. (a) Conversion–time data (■) and kinetic model predictions (—) for an acrylamide polymerization at 50 °C: [monomer] = 3.35 mol/L_2 and $[K_2S_2O_8] = 0.252 \times 10^{-3}$ mol/L_w. (b) Weight-average molecular weight–conversion data (■) and kinetic model predictions (—) for the same experiment.

applicable below 1 ppm with 95% confidence limits of ±0.25%. A CN column (9% groups bonded to a μ-Porasil (silica) substrate, Waters Associates) with a 8-mm i.d. and 4-μm particles was used as the stationary phase. The column was housed in a radial compression system (RCM-100, Waters) and was operated at a nominal pressure of 180 kg/cm². The HPLC system consisted of a degasser (ERC-3110, Erma Optical Works), a Waters U6K injector, a stainless steel filter, and a CN precolumn (Waters). An ultraviolet detector (Beckman 160) with a zinc lamp operating at a wavelength of 214 nm was used to measure the monomer absorption. A Spectra-Physics SP4200 integrator was used to compute peak areas. The mobile phase was a mixture of 50 vol % acetonitrile (Caledon, distilled in glass, UV grade) and 50 vol % double-distilled deionized water, containing 0.005 mol/L of dibutylamine phosphate. The flow rate was 2.0 mL/min. The

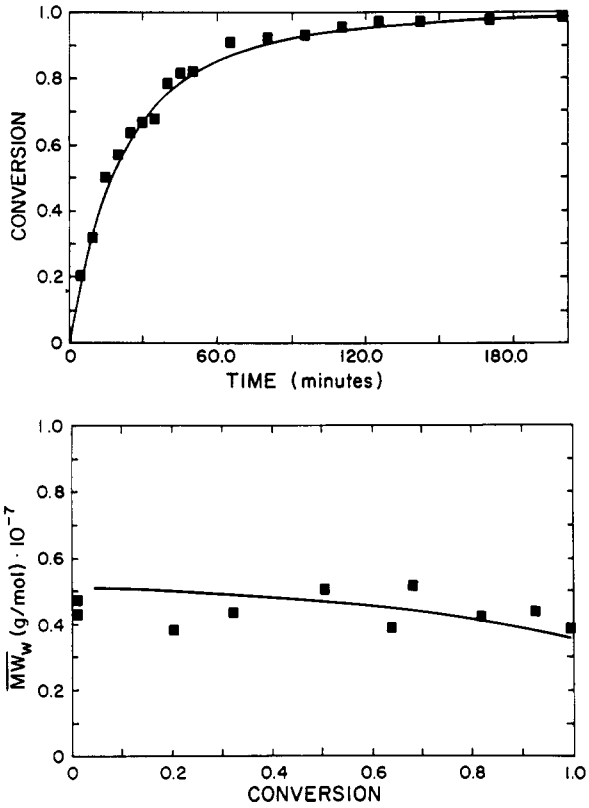

Figure 3. (a) Conversion–time data (■) and kinetic model predictions (—) for an acrylamide polymerization at 50 °C: [monomer] = 4.03 mol/L_w and $[K_2S_2O_8] = 0.228 \times 10^{-3}$ mol/L_w. (b) Weight-average molecular weight–conversion data (■) and kinetic model predictions (—) for the same experiment.

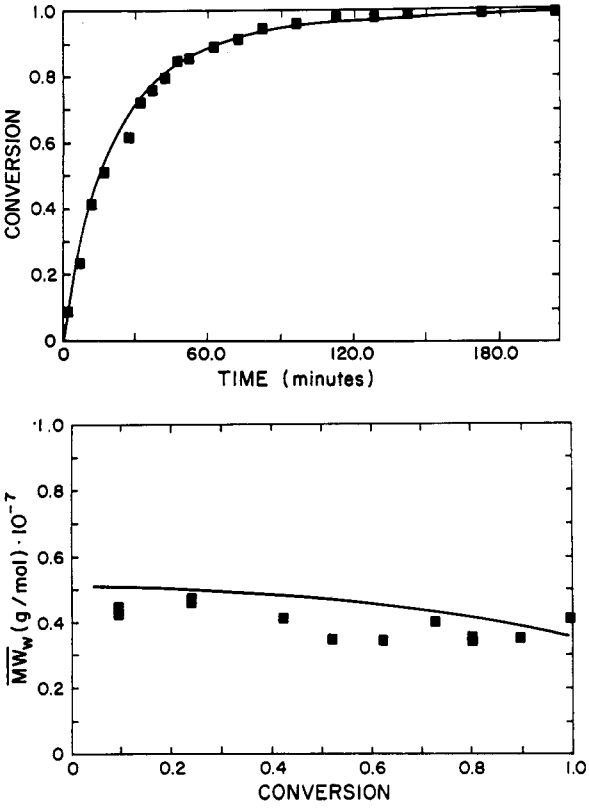

Figure 4. (a) Conversion–time data (■) and kinetic model predictions (—) for an acrylamide polymerization at 50 °C: [monomer] = 4.69 mol/L_w and $[K_2S_2O_8] = 0.251 \times 10^{-3}$ mol/L_w. (b) Weight-average molecular weight–conversion data (■) and kinetic model predictions (—) for the same experiment.

peak separation was optimized by varying the acetonitrile/water ratio.

Molecular weights were measured by using a Chromatix KMX-6 low-angle laser light scattering photometer, with a cell length of 15 mm and a field stop of 0.2. This corresponded to an average scattering angle of 4.8°. A 0.45-μm cellulose/acetate/nitrate filter (Millipore) was used for polymer solutions. A 0.22-μm filter of the same type was used to clarify the solvent. Distilled deionized water with 0.02 M Na_2SO_4 (BDH, analytical grade) was used as a solvent. Weight-average molecular weights were regressed from measurements of the Rayleigh factor using the one-point method.[62] This has been observed to reduce the error in light scattering 2-fold over the conventional dilution procedure.

The refractive index increment of the solvent was determined by using a Chromatix KMX-16 laser differential refractometer at 25 °C and a wavelength of 632.8 nm. The dn/dc was found to be 0.1869.

For polymerizations solid acrylamide monomer (Cyanamid B.V., The Netherlands) was recrystallized from chloroform (Caledon, reagent grade) and washed with benzene (BDH, reagent grade). Potassium persulfate (Fisher Certified, assay 99.5%) was recrystallized from double-distilled deionized water. Both reagents were dried in vacuo to constant weight and stored over silica gel in desiccators.

Method of Polymerization. Polymerization at high monomer concentrations in solutions requires chain-transfer additives to lower molecular weight, reduce viscosity, and provide more efficient heat transfer. However, for this experimental set, chain-transfer agents are undesirable since they can affect the initiation mechanism through redox coupling with persulfate. Therefore, a heterophase water-in-oil polymerization process (inverse microsuspension)[63] was employed. This permitted high aqueous phase monomer concentrations while maintaining a stable, inviscid reaction mixture, ideal for the generation of reliable kinetic data. A prior investigation had demonstrated that inverse-microsuspension and solution polymerization are kinetically equivalent if a water-soluble initiator is employed.[10] In such instances, each isolated monomer droplet contains all reactive species and behaves like a microbatch solution polymerization reactor.

Inverse-microsuspension polymerizations were performed by using Isopar-K (Esso Chemicals) as the continuous phase and sorbitan monostearate (Alkaril Chemicals) as the emulsifier. The aqueous phase consisted of recrystallized acrylamide monomer, distilled deionized water, and recrystallized potassium persulfate. The ratio of aqueous to organic phases was 0.74:1. Polymerizations were performed in a 1-gal stainless steel reactor, continuously agitated at 323 ± 1 rpm. This provided large particle diameters (≈10 μm), which minimized interfacial effects. The reactor was purged with nitrogen (Canadian Liquid Air, UHP grade, 99.999% purity) throughout the polymerization. A complete description of the experimental procedures is given in a prior publication.[61]

Experimental Conditions. Polymerizations were performed isothermally at 40, 50, and 60 °C at monomer concentrations between 25 and 50 wt % of the aqueous phase. The latter corresponding to the solubility limit of acrylamide in water. Table III summarizes the experimental conditions for all polymerizations. For all experiments reactor control was excellent, with thermal deviations never exceeding 1 °C.

Results and Discussion

Rate Order with Respect to Monomer Concentration. The measured residual monomer concentrations were used to calculate the initial rates of polymerization. A series of six experiments were performed at 50 °C with monomer concentrations between 25 and 50 wt % of the aqueous phase, varied in 5% increments. From these data the following rate equation was estimated:

$$R_p \propto M^{1.34\pm0.12}$$

The 95% confidence limits were determined from a nonlinear least-squares estimation routine based on Marquardt's algorithm. The 95% confidence interval sur-

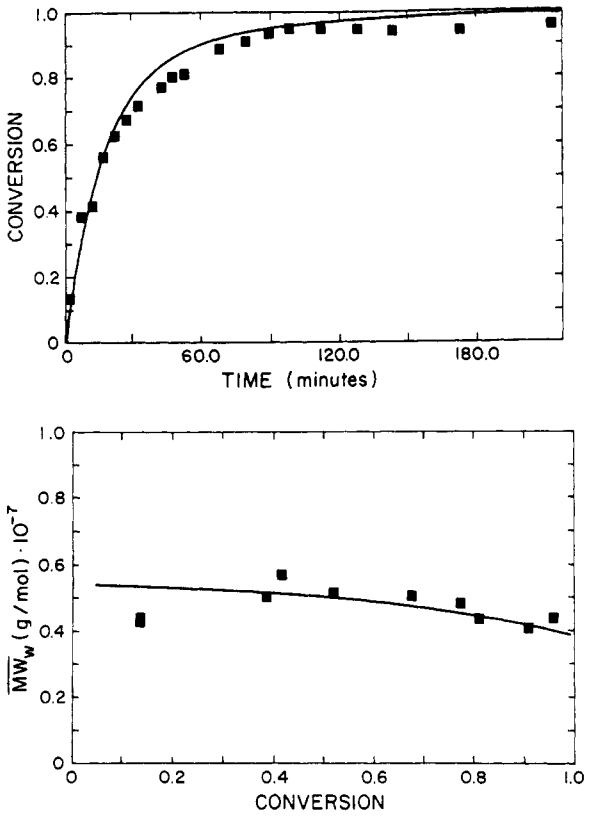

Figure 5. (a) Conversion–time data (■) and kinetic model predictions (—) for an acrylamide polymerization at 50 °C: [monomer] = 5.37 mol/L_w and [$K_2S_2O_8$] = 0.248 × 10^{-3} mol/L_w. (b) Weight-average molecular weight–conversion data (■) and kinetic model predictions (—) for the same experiment.

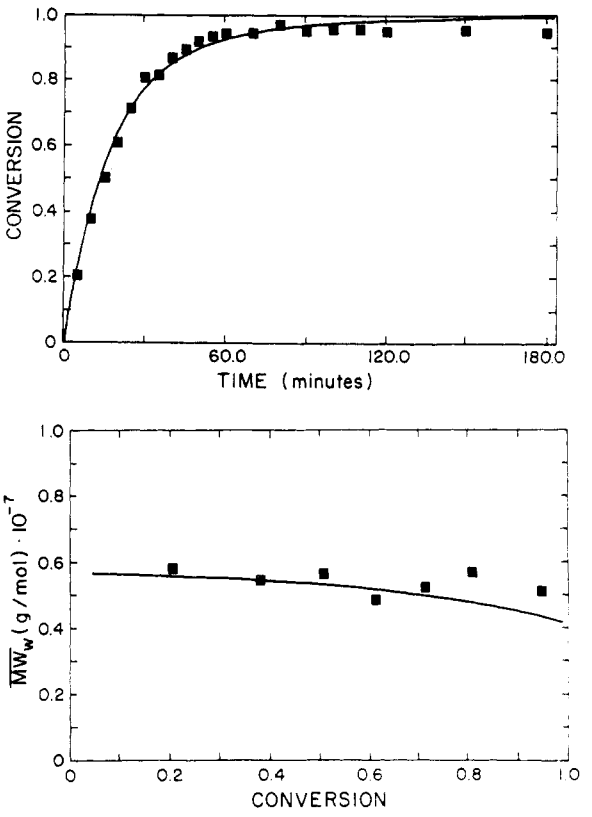

Figure 6. (a) Conversion–time data (■) and kinetic model predictions (—) for an acrylamide polymerization at 50 °C: [monomer] = 6.04 mol/L_w and [$K_2S_2O_8$] = 0.250 × 10^{-3} mol/L_w. (b) Weight-average molecular weight–conversion data (■) and kinetic model predictions (—) for the same experiment.

rounds 1.25, and therefore the hypothesis that at high monomer concentration the rate order deviates from the $^5/_4$th power is rejected. In other words, the rate order with respect to monomer concentration is the same (1.25) from the dilute regime to the solubility limit of acrylamide in water. This has mechanistic implications as it suggests that variable order rate models; the *unmodified* cage-effect and complex theories are not applicable to aqueous persulfate-initiated polymerization of acrylamide. However, the kinetic observations are consistent with the hybrid mechanism, which predicts that the strength of the monomer–initiator association, and hence the rate order, is strictly a function of the chemical composition of the monomer and initiator, independent of the concentration of the reactants. The reliability of the 1.34 order is further accentuated by Kurenkov's recent (1987)[64] result: $R_p \propto M^{1.37}$ for monomer levels between 0.85 and 4.93 mol/L, which has been published after this work began.

Limiting Conversion. During these polymerizations, limiting conversions were observed for several reactions at high monomer or low initiator levels (Table IV). (The usual reciprocal relationship between the limiting conversion and the rate of polymerization[65] has been found in this investigation.) Incomplete monomer consumption is generally attributed to either a depletion of the initiator or isolation of the macroradicals. These phenomena can be distinguished by raising the temperature after the limiting conversion is reached. If residual initiator is present but is physically hindered from reaching the acrylamide monomer, increasing the thermal energy to the system will increase the diffusion of small molecules and increase the rate. Figure 1 shows such an experiment for this system. The temperature rise did not increase the conversion, indicating the initiator concentration had previously been exhausted. Therefore, the limiting conversions offer additional evidence of a second initiator decomposition reaction. Indeed we can conclude the hybrid mechanism is not refuted by the limiting conversion observations. Furthermore, the simultaneous occurrence of limiting conversions in polymerizations with high rate orders with respect to monomer concentration suggests that they are both manifestations of the same phenomena: the formation of hydrogen-bonded associates between acrylamide and potassium persulfate, which leads to the monomer-enhanced decomposition of the initiator.

Parameter Estimation. The conversion–time data were used to estimate two grouped parameters: $\Phi_2 k_a^*$ and f_c (= $1/1 + k_c/k_b$), which are unique to the hybrid mechanism. Additionally, measurements of weight-average molecular weight were used to estimate the transfer to interfacial emulsifier parameter. (Molecular weight development in inverse-microsuspension polymerization has been detailed previously.[61,63]) The differential equations were solved with a variable-order Runge–Kutta procedure with a step size of 1 min.

At each temperature parameter estimates were obtained from a nonlinear least-squares regression routine based on Marquardt's procedure. These estimates were obtained utilizing residual monomer concentration and molecular weight data for all polymerizations at a given temperature. This is preferable to the common practice of estimating parameters from individual experiments, which is unable to identify interexperimental data inconsistencies. This parameter overfitting leads to unreliable estimates, which cannot be generalized to other reaction conditions.

Table V shows the values of parameters determined in this investigation. The activation energy for transfer to

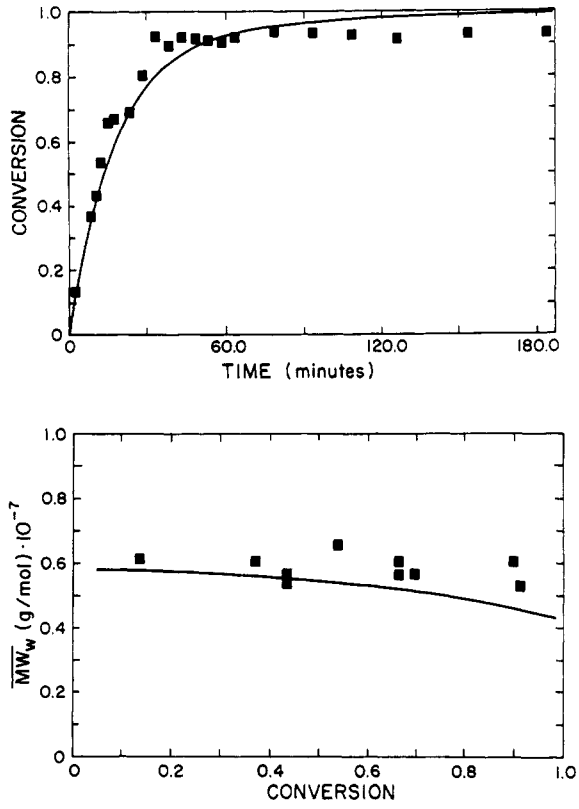

Figure 7. (a) Conversion–time data (■) and kinetic model predictions (—) for an acrylamide polymerization at 50 °C: [monomer] = 6.41 mol/L_w and $[K_2S_2O_8] = 0.238 \times 10^{-3}$ mol/L_w. (b) Weight-average molecular weight–conversion data (■) and kinetic model predictions (—) for the same experiment.

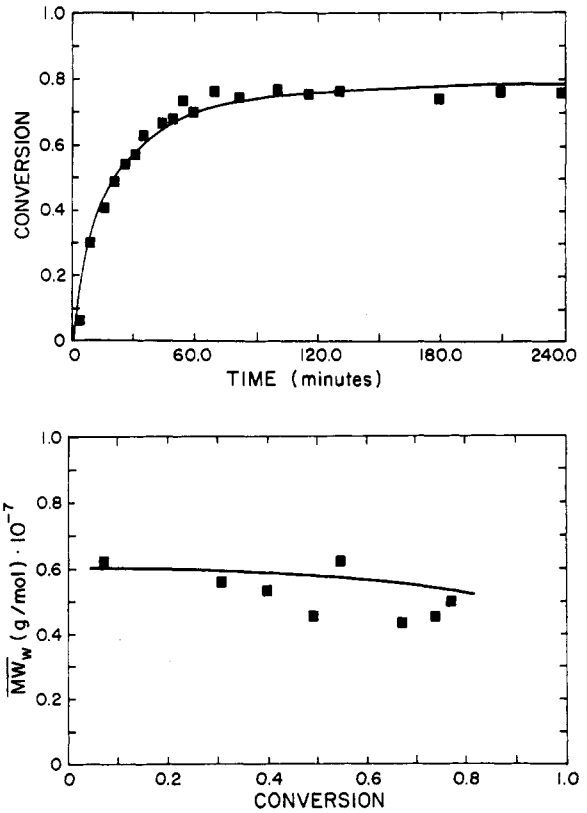

Figure 8. (a) Conversion–time data (■) and kinetic model predictions (—) for an acrylamide polymerization at 60 °C: [monomer] = 6.70 mol/L_w and $[K_2S_2O_8] = 0.0609 \times 10^{-3}$ mol/L_w. (b) Weight-average molecular weight–conversion data (■) and kinetic model predictions (—) for the same experiment.

emulsifier was found to be −141 J/mol, typical of a termination reaction. It was not, however, significantly smaller than zero at the 95% confidence level, and we can conclude that unimolecular termination with interfacial emulsifier is thermally invariant over the range investigated.

The complex–cage efficiency (f_c) is observed to decrease with temperature, implying the monomer-swollen cage preferentially forms inert species rather than active radicals. This is consistent with limiting conversion data, which indicate that initiator deactivation is more favorable at higher temperatures.

The apparent association parameter ($k_a = \Phi_2 k_a^*$) is found to increase with temperature according to an Arrhenius dependence. This has been reported previously for acrylamide polymerizations initiated by potassium persulfate.[9] As was discussed in the derivation of the mechanism, this is the manifestation of two independent phenomena: a decrease in the specific association constant (k_a^*), which is entropically less favorable at elevated temperatures, and an increase in the fraction of potassium persulfate present as diffuse cages (Φ_2). The latter, which is the only form of potassium persulfate capable of participating in monomer-enhanced decomposition reactions, are more abundant at high temperatures due to a greater frequency of radical diffusive displacements and a lower rate of radical fragment recombination. The ability of the hybrid mechanism to quantitatively predict association phenomena, without the thermodynamic inconsistency of the specific association parameter increasing with temperature, is a second major advantage over the unmodified cage-effect and complex theories.

All other rate parameters (k_p, k_{td}, k_{fm}, k_d) were obtained from the literature and have been summarized in a prior publication.[63]

Comparison of Kinetic Model to Experimental Data. Figures 2–9 show conversion–time and weight-average molecular weight–conversion data and model predictions for all experiments. The hybrid mechanism is capable of predicting the initial polymerization rate and weight-average molecular weight well over a range of temperatures, monomer concentrations, and rates of initiation. The molecular weight behavior with conversion is typical of acrylamide polymerizations where transfer to monomer dominates. A slight decrease in molecular weight with conversion (although statistically significant at the 90% confidence level), and the increase with the initial monomer concentration, is evidence that a fraction of the chains are terminated through a bimolecular process. The limiting conversion is also predicted well at low initiator levels and moderate monomer concentrations but, however, is slightly overpredicted when it occurs at very high conversions (>90%). This is due to the authors' personal preference to obtain accurate kinetic parameters at the expense of fitting limiting conversion data. Consequently, initial rate data were given a greater weighting in the analysis to compensate for the larger number of residual monomer measurements at high conversions.

Figure 10 illustrates the relative magnitudes of thermal and monomer-enhanced decomposition of potassium persulfate. At the onset of polymerization the majority of chains are initiated through a donor–acceptor interaction between the acrylamide and persulfate. This effect is most extreme at elevated temperatures. As the conversion rises, both the monomer and initiator have depleted (Figure 11) and thermal bond rupture of the peroxide becomes the predominant initiation reaction. Figure 11 also shows that the rate of consumption of initiator is strongly dependent on the initial monomer concentration. Furthermore, for the conditions of the simulation, the potassium persulfate

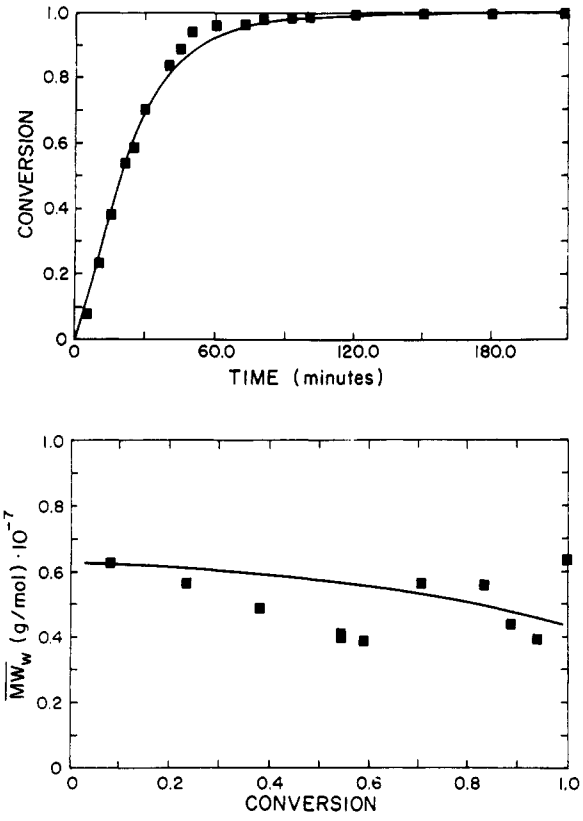

Figure 9. (a) Conversion–time data (■) and kinetic model predictions (—) for an acrylamide polymerization at 40 °C: [monomer] = 6.70 mol/L_w and $[K_2S_2O_8]$ = 1.573 × 10^{-3} mol/L_w. (b) Weight-average molecular weight–conversion data (■) and kinetic model predictions (—) for the same experiment.

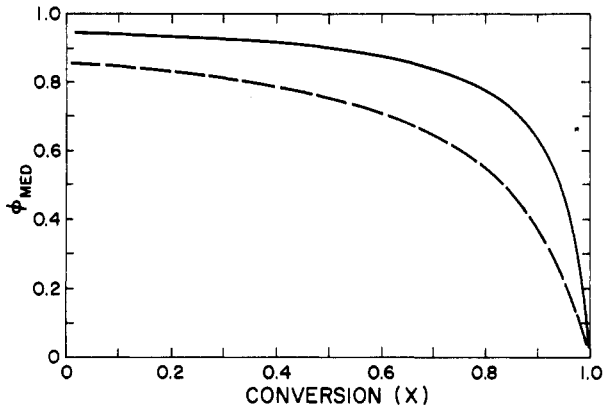

Figure 10. Fraction of polymer chains initiated by monomer-enhanced decomposition of potassium persulfate (Φ_{MED}) as a function of conversion. Simulations were performed at 40 °C (- -) and 60 °C (—) with $[K_2S_2O_8]$ = 6.088 × 10^{-5} mol/L_w, [acrylamide] = 7.04 mol/L_w, and $\Phi_{w/o}$ = 0.74.

is exhausted before the reaction is completed for initial acrylamide concentrations exceeding 25 wt %. For example, at 50 wt % monomer, the radical generation ceases at 78% conversion, in agreement with experimental observations (X_L = 0.76).

Conclusions

The persulfate-initiated polymerization of acrylamide is characterized by the formation of hydrogen-bonded associates between the amide and the persulfate, the decomposition of which proceeds via a donor–acceptor mechanism. The strength and stoichiometry of these associates determine the relative rates of thermal and monomer-enhanced initiation, the rate order of the polymerization with respect to monomer concentration, and the limiting conversion. This association phenomena is observable for any acrylic water-soluble monomer containing electronegative side groups and peroxide-containing initiators and has been included within the framework of a free-radical polymerization mechanism.

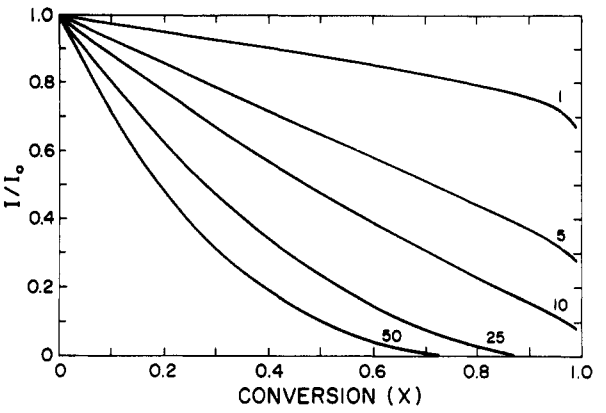

Figure 11. Concentration of potassium persulfate scaled with respect to its initial level (I/I_0) as a function of conversion. Simulations were performed at 60 °C with $[K_2S_2O_8]$ = 2.4 × 10^{-4} mol/L_w and initial acrylamide concentrations of 1, 5, 10, 25, and 50 wt % based on the aqueous phase.

The "hybrid" mechanism offers a significant improvement over existing models for initiation: the cage-effect and complex theories. These incorrectly predict a dependence of the rate order on monomer concentration (found to be invariant to the acrylamide level up to its solubility in water) and contain parameter values that contradict free-energy expectations.

References and Notes

(1) Seymour, K. G.; Harper, B. G. Ger. Pat. 1 197 272, 1965.
(2) Gramain, Ph.; Myard, Ph. *J. Colloid Interface Sci.* **1981**, *84*, 114.
(3) Mowry, D. T.; Hendrick, R. M. U.S. Patent 2 625 471, 1953.
(4) Bikales, N. M. In *Water Soluble Polymers*; Bikales, N. M., Ed.; Plenum Press: New York, 1973; Vol. 2.
(5) Pye, D. J. U.S. Patent 3 072 536, 1963.
(6) Cyanamid, Chemistry of Acrylamide, New Jersey, 1969.
(7) Meltzer, X. L. *Water Soluble Polymers*; Noyes Data Corp.: Park Ridge, NJ, 1979.
(8) Stackman, R. W.; Hurley, S. M. *Polym. Mater. Sci. Eng.* **1987**, *57*, 830.
(9) Riggs, J. P.; Rodriguez, F. *J. Polym. Sci., Polym. Chem. Ed.* **1967**, *5*, 3151.
(10) Hunkeler, D.; Hamielec, A. E. In *Water Soluble Polymers*; Shalaby, S., McCormick, C. L., Butler, G. B., Eds.; American Chemical Society: Washington, DC, 1991.
(11) Riggs, J. P.; Rodriguez, F. *J. Polym. Sci., Polym. Chem. Ed.* **1967**, *5*, 3167.
(12) Jenkins, A. D. *J. Polym. Sci.* **1958**, *29*, 245.
(13) Morgan, L. B. *Trans. Faraday Soc.* **1946**, *42*, 169.
(14) Collinson, E.; Dainton, F. S.; McNaughton, G. S. *Trans. Faraday Soc.* **1957**, *53*, 476.
(15) Collinson, E.; Dainton, F. S.; McNaughton, G. S. *Trans. Faraday Soc.* **1957**, *53*, 489.
(16) Dainton, F. S.; Tordoff, M. *Trans. Faraday Soc.* **1957**, *53*, 499.
(17) Dainton, F. S.; Tordoff, M. *Trans. Faraday Soc.* **1957**, *53*, 666.
(18) Matheson, M. S. *J. Chem. Phys.* **1945**, *13*, 584.
(19) Gee, G.; Rideal, E. K. *Trans. Faraday Soc.* **1936**, *32*, 666.
(20) Cuthbertson, A. C.; Gee, G.; Rideal, E. K. *Proc. R. Soc. London* **1939**, *A170*, 300.
(21) Burnett, G. M.; Loon, L. D. *Trans. Faraday Soc.* **1955**, *51*, 214.
(22) Allen, P. W.; Merrett, F. M.; Scalon, J. *Trans. Faraday Soc.* **1955**, *51*, 95.
(23) Noyes, R. M. *J. Am. Chem. Soc.* **1955**, *77*, 2042.
(24) Stearn, A. E.; Irish, E. M.; Eyring, H. *J. Phys. Chem.* **1940**, *44*, 981.
(25) Ishige, T.; Hamielec, A. E. *J. Appl. Polym. Sci.* **1973**, *17*, 1479.
(26) Flory, P. J. *Principles of Polymer Chemistry*; Cornell University Press: Ithaca, NY, 1953.

(27) Baer, M.; Caskey, J. A.; Fricke, A. L. *Makromol. Chem.* **1972**, *158*, 27.
(28) Hussain, M. M.; Gupta, A. *J. Macromol. Sci., Chem.* **1977**, *A11*, 2177.
(29) Trubitsyna, S. N.; Ismailov, I.; Askarov, M. A. *Vysokomol. Soedin.* **1978**, *A20*, 1624.
(30) Trubitsyna, S. N.; Margaritova, M. F.; Prostakov, N. S. *Vysokomol. soedin.* **1966**, *8*, 532.
(31) Trubitsyna, S. N.; Margaritova, M. F.; Medvedev, S. S. *Vysokomol. Soedin.* **1965**, *7*, 2160.
(32) Trubitsyna, S. N.; Ruzmetova, Kh. K.; Askarov, M. A. *Vysokomol. Soedin.* **1971**, *A13*, 1950.
(33) Trubitsyna, S. N.; Ismailov, I.; Askarov, M. A. *Vysokomol. Soedin.* **1978**, *A20*, 2608.
(34) Morsi, S. E.; Zaki, A. B.; El-Shamy, T. M.; Habib, A. *Eur. Polym. J.* **1976**, *12*, 417.
(35) Bekturov, E. A.; Khamzamulina, R. E. *J. Macromol. Sci., Rev. Macromol. Chem. Phys.* **1987**, *C27*, 253.
(36) Zhuravleva, I. L.; Zav'yalova, Ye. N.; Bogachev, Yu. S.; Gromov, V. F. *Vysokomol. Soedin.* **1986**, *A28*, 873.
(37) Coleman, M. M.; Skrovanek, D. J.; Hu, J.; Painter, P. C. *Polym. Prepr. (Am. Chem. Soc., Div. Polym. Chem.)* **1987**, *28* (1), 19.
(38) Chapiro, A.; Perec-Spritzer, L. *Eur. Polym. J.* **1975**, *11*, 59.
(39) Gromov, V. F.; Galperina, N. I.; Osmanov, T. O.; Khomikovskii, P. M.; Abkin, A. D. *Eur. Polym. J.* **1980**, *16*, 529.
(40) Bune, Ye. V.; Zhuravleva, I. L.; Sheinker, A. P.; Bogachev, Yu. S.; Teleshov, E. N. *Vysokomol. Soedin.* **1986**, *A28*, 1279.
(41) Manickam, S. P.; Venkatarao, K.; Subbaratnam, N. R. *Eur. Polym. J.* **1979**, *15*, 483.
(42) Bunn, D. *Trans. Faraday Soc.* **1946**, *42*, 190.
(43) Chambers, K.; Collinson, E.; Dainton, F. S.; Seddon, W. *Chem. Commun.* **1966**, *15*, 498.
(44) Kolthoff, I. M.; Miller, I. K. *J. Am. Chem. Soc.* **1951**, *73*, 3055.
(45) Osmanov, T. O.; Gromov, V. F.; Komikovsky, P. M.; Abkin, A. D. *Vysokomol. Soedin.* **1978**, *B20*, 263.
(46) Osmanov, T. O.; Gromov, V. F.; Komikovsky, P. M.; Abkin, A. D. *Dokl. Akad. Nauk SSSR* **1978**, *240*, 910.
(47) Misra, G. S.; Rebello, J. J. *Makromol. Chem.* **1974**, *175*, 3117.
(48) Jacob, M.; Smets, G.; DeSchryver, F. C. *J. Polym. Sci.* **1972**, *B10*, 669.
(49) Ergozhin, E. E.; Tausarova, B. R.; Sariyeva, R. B. *Makromol. Chem., Rapid Commun.* **1987**, *8*, 171.
(50) Haas, H. C.; MacDonald, R. L.; Schuler, A. N. *J. Polym. Sci., Polym. Chem. Ed.* **1970**, *8*, 1213.
(51) Gupta, K. C.; Lai, M.; Behari, K. *Polym. Prepr. (Am. Chem. Soc., Div. Polym. Chem.)* **1987**, *28* (1), 118.
(52) Manickam, S. P.; Subbaratnam, N. R.; Venkatarao, K. *J. Polym. Sci., Chem.* **1980**, *18*, 1679.
(53) Burfield, D. R.; Ng, S. C. *Eur. Polym. J.* **1976**, *12*, 873.
(54) Kurenkov, V. F.; Myagchenkov, V. A. *Eur. Polym. J.* **1980**, *16*, 1229.
(55) Jaeger, W.; Hahn, M.; Seehaus, F.; Reinisch, G. *J. Macromol. Sci., Chem.* **1984**, *A21*, 593.
(56) Hahn, M.; Jaeger, W.; Reinisch, G. *Acta Polym.* **1983**, *34*, 322.
(57) Hahn, M.; Jaeger, W.; Reinisch, G. *Acta Polym.* **1983**, *35*, 350.
(58) Friend, J. P.; Alexander, A. E. *J. Polym. Sci., Polym. Chem. Ed.* **1968**, *6*, 1833.
(59) Trubitsyna, S. N.; Ismailov, I.; Askarov, M. A. *Vysokomol. Soedin.* **1977**, *A19*, 495.
(60) Hunkeler, D.; Hamielec, A. E.; Baade, W. In Polymerization of Cationic Monomers with Acrylamide. *Polymers in Aqueous Media: Performance through Association*; Glass, J. E., Ed.; American Chemical Society, Washington, DC, 1989.
(61) Hunkeler, D. Ph.D. Dissertation, McMaster University: Hamilton, Canada, 1990.
(62) Hunkeler, D.; Hamielec, A. E. *J. Appl. Polym. Sci.* **1988**, *35*, 1603.
(63) Hunkeler, D.; Hamielec, A. E.; Baade, W. *Polymer* **1989**, *30*, 127.
(64) Kurenkov, V. F.; Baiburdov, T. A.; Stupen'kova, L. L. *Vysokomol. Soedin.* **1987**, *A29*, 348.
(65) Joshi, M. G.; Rodriguez, F. *J. Polym. Sci., Chem.* **1988**, *26*, 819.

Registry No. $K_2S_2O_8$, 7727-21-1; acrylamide, 79-06-1.